

# RF Pulse Design for Parallel Excitation

Douglas C. Noll<sup>1</sup>, William A. Grissom<sup>1</sup>, Chun-yu Yip<sup>2</sup>

Departments of <sup>1</sup>Biomedical Engineering and <sup>2</sup>Electrical Engineering and Computer Science  
University of Michigan, Ann Arbor, MI USA

## 1. Introduction

Parallel excitation has been introduced as a means of accelerating multi-dimensional, spatially-selective excitation using multiple transmit coils, each driven by a unique RF pulse (1,2). In a manner analogous to parallel imaging, parallel excitation allows the use of a reduced excitation k-space trajectory (7) to achieve a desired excitation pattern, by exploiting the blurring effect of coil sensitivity patterns in the excitation k-space domain to deposit RF energy in regions not traversed by the trajectory. Proposed applications include the shortening of multi-dimensional RF pulses for  $B_1$  and  $B_0$  inhomogeneity compensation (8-11), and Specific Absorption Rate (SAR) management (2). The feasibility of parallel excitation has also recently been verified experimentally in (12,13).

In this paper we present a review of RF pulse design methods for parallel excitation and demonstrate their application. The pioneering methods were introduced by Katscher, et al. (1) and by Zhu (2). The method by Katscher, et al. (1) is characterized by the explicit use of transmit sensitivity patterns in the pulse design process, and its formulation is based on a convolution in excitation k-space. It allows usage of arbitrary k-space trajectories. Grissom, et al. (3) proposed an RF pulse design technique that is closely related to Katscher's method, but is formulated in the spatial domain. It is a multi-coil generalization of the iterative pulse design method proposed by Yip, et al. (14). The method introduced by Zhu also makes explicit use of transmit sensitivity patterns and is formulated as an optimization problem in the spatial domain, and, as presently described, is restricted to Cartesian (e.g. echo-planar) k-space trajectories. Griswold, et al. (4) proposed a k-space domain method that is analogous to GRAPPA imaging (6). It is unique in that it does not require prior determination of sensitivity patterns. Instead, it involves an extra calibration step in the pulse design process. It also appears to be restricted to Cartesian k-space trajectories. All of the aforementioned design approaches are based on the assumption of small-tip-angle excitation.

In the following section we review the formulations of the four RF pulse design approaches in detail. We then present a discussion of applications of parallel excitation, including the acceleration of multi-dimensional selective excitation pulses,  $B_1$  inhomogeneity compensation, and SAR management.

## 2. Current RF Pulse Design Methods for Parallel Excitation

### 2.A. Spatial Domain Approach

The design approach introduced by Grissom et al (3) is formulated as an optimization problem in the spatial domain. Exploiting linearity in the small-tip regime (7), the aggregate transverse excitation pattern produced by  $C$  transmit coils can be approximated by a weighted summation of  $C$  Fourier integrals along a k-space trajectory (11),  $\mathbf{k}(t) = [k_x(t) \quad k_y(t) \quad k_z(t)]^T$ , that are temporally weighted by unique complex RF pulses  $b_c(t)$ . The  $c$ -th integral is spatially weighted by the complex transmit sensitivity pattern  $s_c(\mathbf{x})$  for coil  $c$ :

$$m(\mathbf{x}) = i\gamma m_0 \sum_{c=1}^C s_c(\mathbf{x}) \int_0^T b_c(t) e^{i\gamma \Delta B_0(\mathbf{x})(t-T)} e^{i\mathbf{x} \cdot \mathbf{k}(t)} dt. \quad [1]$$

In this equation,  $\gamma$  is the gyromagnetic ratio,  $m_0$  is the equilibrium magnetization magnitude,  $T$  is the pulse length, and  $e^{i\gamma \Delta B_0(\mathbf{x})(t-T)}$  represents the phase accrued due to main field deviation  $\Delta B_0(\mathbf{x})$ . The method places no restrictions on the choice of trajectory  $\mathbf{k}(t)$ , defined as the time-reversed integral of the gradient waveforms (7). Discretizing time to  $N_t$  samples and space to  $N_s$  samples, we may write:

$$\mathbf{m} = \sum_{c=1}^C \text{diag}\{s_c(\mathbf{x}_i)\} \mathbf{A} \mathbf{b}_c, \quad [2]$$

where  $\mathbf{b}_c$  is a length- $N_t$  vector of RF pulse samples for coil  $c$ , and  $\mathbf{m}$  is the length- $N_s$  vector of spatial samples of the aggregate excitation pattern. The  $(i, j)$ -th element of the  $N_s \times N_t$  system matrix  $\mathbf{A}$  is given by:

$$a_{ij} = i\gamma m_0 \Delta t e^{i\gamma \Delta B_0(\mathbf{x}_i)(t_j - T)} e^{i\mathbf{x}_i \cdot \mathbf{k}(t_j)}. \quad [3]$$

Equation [2] can be rewritten via horizontal concatenation of the matrices  $\text{diag}\{s_c(\mathbf{x}_i)\} \mathbf{A}$  and vertical concatenation of the vectors  $\mathbf{b}_c$ , resulting in:

$$\mathbf{m} = \left[ \text{diag}\{s_1(\mathbf{x}_i)\} \mathbf{A} \quad \cdots \quad \text{diag}\{s_C(\mathbf{x}_i)\} \mathbf{A} \right] \begin{bmatrix} \mathbf{b}_1 \\ \vdots \\ \mathbf{b}_C \end{bmatrix} = \mathbf{A}_{full} \mathbf{b}_{full}. \quad [4]$$

Given a vector  $\mathbf{m}_{des}$  containing  $N_s$  samples of a desired pattern at spatial locations  $\{\mathbf{x}_i\}_{i=1}^{N_s}$ , the RF pulses can be designed via solving the following minimization problem:

$$\hat{\mathbf{b}}_{full} = \arg \min_{\mathbf{b}_{full}} \left\{ \left\| \mathbf{A}_{full} \mathbf{b}_{full} - \mathbf{m}_{des} \right\|_{\mathbf{W}}^2 + R(\mathbf{b}_{full}) \right\}, \quad [5]$$

where  $\mathbf{W}$  is an  $N_s \times N_s$  diagonal matrix containing an error weighting that one can use to specify spin-free regions as “don’t-care” regions. In general, it is beneficial to define  $\{\mathbf{x}_i\}_{i=1}^{N_s}$  as a spatial grid of finer resolution than that supported by the accelerated trajectory, in order to produce smooth excitation in continuous space (14). The minimization problem can be solved by brute-force inversion or efficiently by the CG method, in a manner similar to the single-coil pulse design method (14).

## 2.B. Transmit SENSE Approach

In contrast to the previously described spatial-domain method, the design approach formulated by Katscher, et al. (1), coined “transmit SENSE,” is formulated in the frequency, or k-space domain. Assuming small tip angles (7), the Fourier transform of the aggregate excitation pattern  $\mathbf{m}(\mathbf{x})$  resulting from simultaneous excitation by  $C$  coils is given by:

$$p(\mathbf{k}) = \sum_{c=1}^C S_c(\mathbf{k}) \otimes p_c(\mathbf{k}), \quad [6]$$

where  $S_c$  is the Fourier transform of the transmit sensitivity pattern of coil  $c$ ,  $p_c$  is the Fourier transform of the excitation pattern produced by coil  $c$ , and the operator  $\otimes$  denotes a convolution. This equation can be discretized in  $\mathbf{k}$ , forming a length- $N_s$  vector  $\mathbf{p}$  that contains samples along a fully sampled grid  $\{\mathbf{k}_s\}_{s=1}^{N_s}$ ,  $C$  circulant convolution matrices  $\mathbf{S}_c$  of size  $N_s \times N_t$ , and  $C$  length- $N_t$  vectors  $\mathbf{p}_c$  containing samples along a common accelerated trajectory  $\{\mathbf{k}_t\}_{t=1}^{N_t}$ . In general, there are no restrictions placed on the choice of the fully sampled grid and the accelerated trajectory, though for simplicity the fully sampled grid  $\{\mathbf{k}_s\}_{s=1}^{N_s}$  is generally Cartesian. The circulant convolution matrices  $\mathbf{S}_c$  may be constructed by taking the discrete Fourier transform of the measured transmit sensitivity patterns, and interpolating each onto a grid of points given by  $(\mathbf{k}_s - \mathbf{k}_t)$ . The result of the discretization procedure is a sum of matrix/vector products given by:

$$\mathbf{p} = \sum_{c=1}^C \mathbf{S}_c \mathbf{p}_c. \quad [7]$$

We may replace the summation in Eq. 2 by concatenating the  $C$  convolution matrices to form the size- $N_s \times C \cdot N_t$  matrix  $\mathbf{S}_{full}$ , and concatenating the transforms of the excitation patterns, resulting in the length- $CN_t$  vector  $\mathbf{p}_{full}$ :

$$\mathbf{p} = \begin{bmatrix} \mathbf{S}_1 & \cdots & \mathbf{S}_C \end{bmatrix} \begin{bmatrix} \mathbf{p}_1 \\ \vdots \\ \mathbf{p}_C \end{bmatrix} = \mathbf{S}_{full} \mathbf{p}_{full}. \quad [8]$$

A regularized least-squares cost function can then be defined and minimized to yield the Fourier transforms of the individual coils' excitation patterns:

$$\hat{\mathbf{p}}_{full} = \arg \min_{\mathbf{p}_{full}} \left\{ \left\| \mathbf{S}_{full} \mathbf{p}_{full} - \mathbf{p}_{des} \right\|^2 + R(\mathbf{p}_{full}) \right\}, \quad [9]$$

where  $\mathbf{p}_{des}$  is a vector containing  $N_s$  samples of the Fourier transform of the desired excitation pattern, and  $R(\mathbf{p}_{full})$  denotes a general regularization term. The RF pulse for coil  $c$ ,  $\mathbf{b}_c$ , can be derived from  $\mathbf{p}_c$  by multiplication with the Jacobian determinant for k-space density and velocity compensation (1).

### 2.C. Regularization in Spatial Domain and Transmit SENSE Methods

Both the transmit SENSE and the spatial-domain methods are formulated with regularization terms  $R(\cdot)$  that provide design control over pulse characteristics such as integrated RF power, peak RF power, and waveform smoothness (Equations 5 and 9). In the spatial-domain method,  $R(\mathbf{b}_{full})$  operates directly on the RF samples, and in transmit SENSE,  $R(\mathbf{p}_{full})$  operates on the frequency-domain excitation patterns, from which RF samples can be obtained via multiplication with a diagonal matrix containing k-space density and velocity compensation terms. In the spatial-domain method, integrated RF power may be controlled via a Tikhonov regularization term  $R(\mathbf{b}_{full}) = \beta \mathbf{b}'_{full} \mathbf{b}_{full}$ , where prime denotes complex conjugate transpose, and  $\beta$  is a tuning parameter. This term is useful for controlling SAR, as it reduces the time-averaged RF power. Instantaneous RF power is controlled via  $R(\mathbf{b}_{full}) = \mathbf{b}'_{full} \Lambda \mathbf{b}_{full}$ , where  $\Lambda = \text{diag}\{\lambda_j\}$ , with  $\lambda_j, j = 0, \dots, C \cdot N_t - 1$  denoting regularization parameters used to control the magnitude of individual RF pulse samples. Regularization on instantaneous RF power is useful for suppressing waveform peaks, so that the waveforms can be scaled to produce larger tip angles within the limit of the amplifier. Both regularization on integrated and instantaneous RF power are useful for mitigating increased excitation error as RF pulses are scaled to achieve large tip angles. Waveform smoothness can be tuned via  $R(\mathbf{b}_{full}) = \alpha \mathbf{b}'_{full} \mathbf{C} \mathbf{b}_{full}$ , where  $\mathbf{C}$  is a finite-differencing matrix.

### 2.D. Removal of Aliasing Approach

In an approach developed by Zhu (2), one considers the aliasing pattern in the spatial domain that results from undersampling of the excitation k-space trajectory, and solves for the necessary excitation patterns for each coil. For example, consider the case of a two-dimensional Cartesian trajectory with undersampling along the  $y$  dimension. The aggregate excitation pattern can be expressed as:

$$m(x, y) = \sum_{c=1}^C s_c(x, y) \sum_{m=-\infty}^{\infty} u_c(x, y - m\Delta), \quad [10]$$

where  $u_c$  is the excited pattern for  $c^{\text{th}}$  coil using the fully sampled excitation k-space trajectory and  $\Delta = FOV / R$  is the spacing of the aliasing for speedup factor  $R$ . If we consider solutions in the form  $u_c(x, y) = h_c(x, y) m_{des}(x, y)$ , then equation [10] can be rewritten as:

$$m(x, y) = \sum_{m=-\infty}^{\infty} m_{des}(x, y - m\Delta) \sum_{c=1}^C h_c(x, y - m\Delta) s_c(x, y). \quad [11]$$

One can see that the excited pattern can be made equal to the desired pattern if over the FOV:

$$\sum_{c=1}^C h_c(x, y - m\Delta) s_c(x, y) = \begin{cases} 1, & m = 0 \\ 0 & \text{otherwise} \end{cases}. \quad [12]$$

Thus, for each point  $(x, y)$  in the FOV, we can construct the following matrix equation:

$$\begin{bmatrix} s_1(x, y) & s_2(x, y) & \cdots & s_C(x, y) \\ \vdots & & \ddots & \vdots \\ s_1(x, y + m\Delta) & s_2(x, y + m\Delta) & \cdots & s_C(x, y + m\Delta) \\ \vdots & & & \vdots \end{bmatrix} \begin{bmatrix} h_1(x, y) \\ h_2(x, y) \\ \vdots \\ h_C(x, y) \end{bmatrix} = \begin{bmatrix} 1 \\ 0 \\ \vdots \\ 0 \end{bmatrix}, \quad [13]$$

which is a system of  $R$  equations with  $C$  unknowns (typically  $R \leq C$ ). Least-squares solutions to [13] can be obtained via pseudo-inverse or other methods, yielding the appropriate excitation pattern for each coil,  $u_c(x, y) = h_c(x, y) m_{des}(x, y)$ , which can then be used to calculate the RF pulse using the excitation k-space perspective under small-tip-angle approximation (7).

It should be noted that this formalism is very similar to the solution of the receive SENSE problem using an undersampled Cartesian trajectory (5). Similar to SENSE, the number of equations in [13] can be less than  $R$  at spatial locations where, due to object shape, there are fewer than  $R$  excitation pattern replicas overlapping at those locations. Likewise, if a more complex undersampling pattern is used (for example, in three-dimensional parallel excitation), then a more complex pattern of overlapping aliasing can be incorporated into this expression, albeit leading to larger matrices to be inverted.

### 2.E. Issues Associated with Determination of Transmit Patterns

The above three design methods all assume knowledge of the transmit sensitivity patterns,  $s_c(\mathbf{x})$ . These quantities are analogous to receive sensitivity patterns in parallel imaging, and their accurate determination is important for excitation accuracy. One way to estimate  $s_c(\mathbf{x})$  is to obtain relative excitation patterns by playing out a common RF pulse on each coil individually and collecting images with a fixed receiver system (using single channel or parallel acquisition). The relative phase of  $s_c(\mathbf{x})$  can be determined by examining the relative phase between these images. Similarly, relative amplitudes can be determined by examining the amplitude of the response for each coil. However, to excite a target flip angle exactly, one must have knowledge of the absolute  $B_1$  field amplitude per unit current in the coil, which may be obtained by applying a  $B_1$ -mapping method to each transmit coil (22-24).

Finally, there is the issue of mutual inductance between coils. One can attempt to eliminate the effects of mutual inductance between the coils (25,26), or allow the mutual inductance to occur and account for it in the pulse design (2). In the latter case, the effective sensitivity pattern of the  $r$ -th coil can be modeled by a weighted sum over all sensitivity patterns:

$$\hat{s}_r(\mathbf{x}) = \sum_{c=1}^C \gamma_{r,c} s_c(\mathbf{x}), \quad [14]$$

where  $\gamma_{r,c}$  accounts for the coupling between coils  $r$  and  $c$ .

### 2.F. Pulse Design without Explicit Determination of Transmit Patterns

In contrast to the previous three methods, Griswold et al. (4) have suggested an approach to designing parallel excitation pulses, known as transmit GRAPPA, which does not require the determination of transmit sensitivity patterns. In a manner analogous to receive GRAPPA (6), the method requires calibration of k-space data that are acquired using segments of a common RF pulse prior to the actual transmit GRAPPA experiment. As in Zhu's method, it is assumed that the excitation k-space trajectory is Cartesian and is accelerated in one dimension by a speed-up factor  $R$ . It is also assumed that a relatively uniform  $B_1$  field may be produced via simultaneous excitation on all coils. For example, this may require that, for a circular array of transmit coils, the default coil phase varies with angular position so as to produce an approximation to circular polarization. The method begins with an initial 2D RF pulse, designed using standard methods (7), that produces a desired excitation pattern  $m_{des}$  using a fully

sampled k-space trajectory and uniform transmit sensitivity. Considering the aforementioned assumption of a uniform  $B_1$ -field when using all coils, the desired pattern  $m_{des}$  can be excited by playing out the initial pulse on all coils simultaneously. The initial pulse can be decomposed into its undersampled parts by taking every  $R$ -th line in excitation k-space:  $b^{full}(k_x, k_y) = \sum_{r=1}^R b^r(k_x, k_y)$ . Let  $m_c^r(x, y)$  be the pattern excited by the  $c^{\text{th}}$  coil with the pulse corresponding to the  $r$ -th k-space segment,  $b^r(k_x, k_y)$  and let the aggregate pattern for all coils produced by simultaneous excitation along the  $r$ -th k-space segment be  $m^r(x, y) = \sum_{c=1}^C m_c^r(x, y)$ . It follows that the combined excitation along all segments and across all coils will produce the desired pattern:

$$m_{des}(x, y) = \sum_{r=1}^R m^r(x, y). \quad [15]$$

The basic idea in transmit GRAPPA is to determine what weighted combination of RF pulses, transmitted along a single k-space segment (e.g.  $r = 1$ ), will produce  $m_{des}$ .

More specifically, the design method will attempt to determine what RF pulses for each of the coils, transmitted along segment  $r = 1$ , will produce the other segments' excitation patterns,  $m^r(x, y)$ ,  $r = 2, \dots, R$ . Thus, the  $m^r(x, y)$  represent the *targets* of the parallel excitation scheme and are half of the required calibration data for transmit GRAPPA. These target patterns,  $m^r(x, y)$ , are determined experimentally by transmitting pulse segment  $b^r$  to all coils simultaneously. This acquisition is repeated for excitation along all segments  $r = 2, \dots, R$ . Next, calibration data representing the *building blocks* for exciting  $m^r(x, y)$  must also be obtained. As a matter of convenience, one can choose the first segment of the initial pulse  $b^1$  as the building block. By exciting this pulse individually on each of the  $C$  coils, one can acquire  $m_c^1(x, y)$ , which form the other half of required calibration data. If necessary, one can excite a richer set of building blocks, the use of which may yield a more accurate fit to the target k-space data. Finally, the relationship between the segment one excitation patterns ( $m_c^1(x, y)$ ) and the target patterns ( $m^r(x, y)$ ) is determined to build the final RF pulses. In practice, this relationship is examined in the k-domain and, in a manner similar to receive GRAPPA, a linear combination of RF pulses from the individual coils (the building blocks) with shifts in k-space form the pulses that produce the pattern for each target segment,  $m^r(x, y)$ .

The final RF pulses will be in the form:

$$\tilde{b}_c^r = \sum_{r=1}^R \tilde{b}_c^r, \quad [16]$$

where  $\tilde{b}_c^r$ ,  $c = 1, \dots, C$ , is the set of RF pulses that, when transmitted simultaneously along segment 1, will produce the excitation pattern for segment  $r$ ,  $m^r(x, y)$ . By equation [15], simultaneous transmission of  $\tilde{b}_c^r$ ,  $c = 1, \dots, C$ , will produce  $m_{des}$ . The subpulses  $\tilde{b}_c^r$  are constructed from weighted combinations of shifted versions of the *building block* RF pulse:

$$\tilde{b}_c^r(k_x, k_y) = \sum_{p, q} a_c^r(p, q) b^1(k_x - p\Delta k, k_y - qR\Delta k), \quad [17]$$

where  $p$  and  $q$  map out a neighborhood in excitation k-space and  $a_c^r(p, q)$  are the GRAPPA coefficients. As with receive GRAPPA, the underlying assumption is that the transmit patterns blur the RF pulses into

neighboring lines in k-space. The GRAPPA coefficients are determined by finding the coefficients that best fit the following relationship:

$$M^r(k_x, k_y) = \sum_{c=1}^C \sum_{p,q} a_c^r(p,q) M_c^1(k_x - p\Delta k, k_y - qR\Delta k), \quad [18]$$

where  $M^r$  and  $M_c^1$  are the acquired k-space data associated with the calibration excitation patterns  $m^r$ ,  $r = 2, \dots, R$ , and  $m_c^1$ ,  $c = 1, \dots, C$ . Thus, the coefficients that are used to construct the *target* RF pulses from the *building block* RF pulses are obtained from a fitting procedure that is performed on images of the excitation patterns that the target and building block pulses produce. The method therefore obviates the need for estimates of transmit sensitivity patterns, because they are manifest in the linear transformation from RF pulses to excitation patterns. Interestingly, while the shifts in equation [17] are in excitation k-space and the shifts in equation [18] are in acquisition k-space, these shifts are the same provided the field of view of the acquired data and the initial fully-sampled RF pulse is the same. Thus, only a few acquisition lines are necessary to determine the transmit GRAPPA coefficients.

### 3. Applications of Parallel Excitation

#### 3.A. General Multi-dimensional RF Pulse Acceleration

Compared to multi-dimensional excitation with a single volume coil, parallel RF transmission with localized coils allows for a reduction of pulse length. The reduction comes from the possible use of an undersampled k-space trajectory with an excitation FOV (XFOV) smaller than the FOV of the desired pattern. This ability to use such a trajectory arises from the blurring effect of transmit sensitivity patterns in the frequency domain, which spreads RF energy into k-space regions not traversed by the undersampled trajectory. In analogy to parallel imaging, we can characterize the reduction by a *speedup factor*, defined as the ratio of the FOV of the desired excitation pattern to the XFOV of the undersampled trajectory. High excitation accuracy can be maintained over a range of speedup factors in parallel transmission, as demonstrated in Figure 1, which shows simulated images corresponding to no acceleration (Fig 1a), and a speedup factor of 4 (Fig 1b). The parallel transmit simulation assumed an eight-channel head transmit array, and both pulse sets were designed to excite a rectangular block of flip angle 10 degrees inside a circular ROI, using spiral trajectories with different XFOV. From these images and their corresponding excitation error it is evident that excitation accuracy is maintained despite a reduction in pulse length from 7.2ms to 2.1ms.

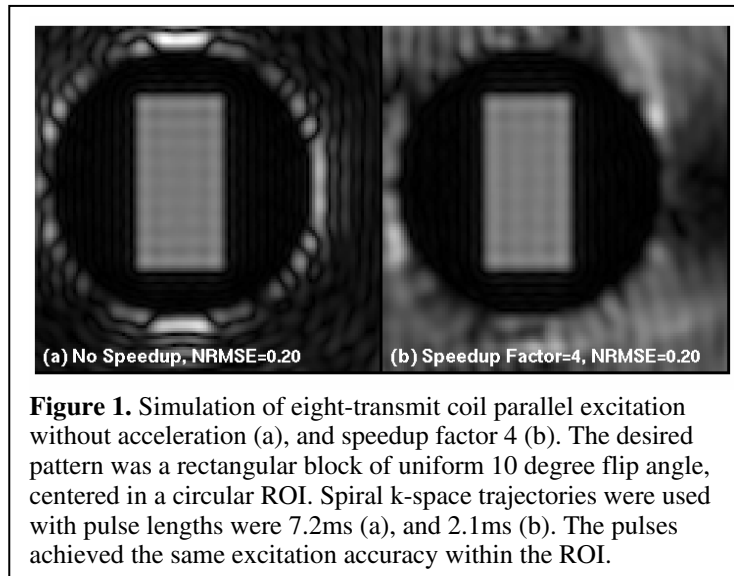


**Figure 1.** Simulation of eight-transmit coil parallel excitation without acceleration (a), and speedup factor 4 (b). The desired pattern was a rectangular block of uniform 10 degree flip angle, centered in a circular ROI. Spiral k-space trajectories were used with pulse lengths were 7.2ms (a), and 2.1ms (b). The pulses achieved the same excitation accuracy within the ROI.

#### 3.B. $B_1$ Inhomogeneity Compensation

The problem of  $B_1$  inhomogeneity in MRI at high fields is well known. Stenger et al (8) have recently proposed the application of parallel excitation to the shortening of multi-dimensional selective excitation pulses for  $B_1$  inhomogeneity compensation. Parallel excitation is well suited to this problem because  $B_1$  inhomogeneity is captured as a feature of the measured transmit sensitivity patterns. Thus a homogeneous excitation may be achieved with RF pulses designed using these sensitivity patterns and a homogeneous desired excitation pattern. Figure 2b shows an experimental image obtained at 3T, demonstrating the use of parallel excitation for  $B_1$  inhomogeneity compensation. Pulses in this experiment

were designed using a ‘fast- $k_z$ ’ trajectory (27) and the spatial domain method proposed by Grissom et al. The experiment was performed using the reciprocity-based method described in (17). It can be seen that parallel excitation using these pulses results in a more homogeneous excitation (Fig 2b) than excitation using a standard slice-selective excitation with multiple transmitters (Fig 2a).

### 3.C. SAR Management

Zhu (2) has shown that parallel excitation can be employed for the purpose of SAR management, which is of great concern at high field strengths. In a given parallel excitation experiment, assuming that the speedup factor  $R$  is less than the number of coils  $C$ , equations [5], [9], [13], and [18], which are the design equations central to each approach, are underdetermined problems. In each case, there are fewer constraint equations than variables, and there exists a family of RF pulse solutions, all of which yield equally good excitation error. It then becomes feasible to employ an additional metric in the design process to favor RF pulses with low average SAR. For example, SAR may be quantified as:

$$SAR_{ave} = \mathbf{b}'_{full} \mathbf{F} \mathbf{b}_{full}, \quad [19]$$

The matrix  $\mathbf{F}$  in [19] relates the RF pulse samples to the squared absolute value of the electric fields in the sample, and is based on the application of quasi-static approximations to Maxwell’s equations, whereby it may be assumed that the electric field in the sample volume scales linearly with the applied current in the coils. Such a metric might be employed in the RF pulse design process by enforcing a maximum allowable norm-squared excitation error  $\varepsilon_{max}$ , while minimizing with respect to average SAR. To achieve this, the spatial domain design method could be modified as:

$$\hat{\mathbf{b}}_{full} = \arg \min_{\mathbf{b}_{full}} \{ \mathbf{b}'_{full} \mathbf{F} \mathbf{b}_{full} \},$$

$$\text{subject to: } \left\| \mathbf{A}_{full} \hat{\mathbf{b}}_{full} - \mathbf{m}_{des} \right\|_{\mathbf{W}}^2 \leq \varepsilon_{max}, \quad [20]$$

which is a nonlinear optimization problem in  $\mathbf{b}_{full}$ . Zhu (2) reported a 38% decrease in average SAR between RF pulses designed by minimizing excitation error alone and pulses designed in a nonlinear fashion, as in [20], for a nine-channel transmit array with speedup factor 4.

### 4. Summary

Parallel excitation is a burgeoning technology with the potential to alleviate several problems in MR imaging, particularly those arising at high field strengths. In this work, we have presented a theoretical overview of four current RF pulse design approaches in parallel excitation, and have discussed practical details concerning their implementation. We have also presented a discussion of three applications of parallel excitation, namely general multidimensional RF pulse acceleration,  $B_1$  inhomogeneity compensation, and SAR management.

### 5. References

1. Katscher U, Bornert P, Leussler C, van den Brink JS. Transmit SENSE. Magn Reson Med 2003;49(1):144-150.
2. Zhu Y. Parallel excitation with an array of transmit coils. Magn Reson Med 2004;51(4):775-784.
3. Grissom W, Yip CY, Noll DC. An Image Domain Approach for the Design of RF Pulses in Transmit SENSE. In: Proceedings of the 13<sup>th</sup> Annual Meeting of ISMRM, 2005; Miami. p 19.
4. Griswold M, Kannengiesser S, Muller M, Jakob P. Autocalibrated Accelerated Parallel Excitation

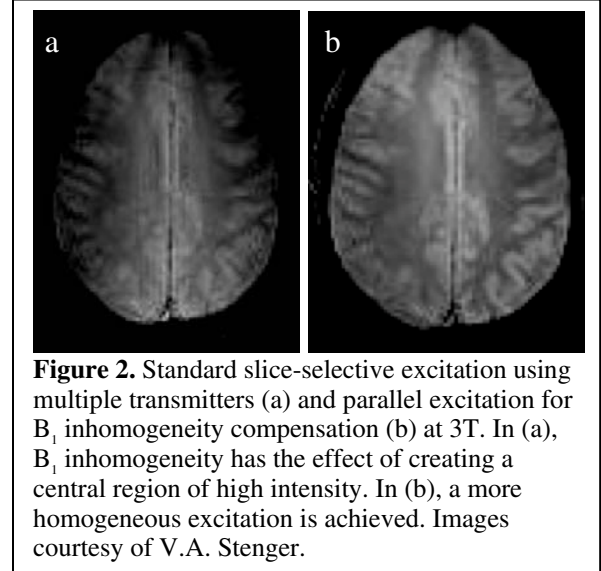


**Figure 2.** Standard slice-selective excitation using multiple transmitters (a) and parallel excitation for  $B_1$  inhomogeneity compensation (b) at 3T. In (a),  $B_1$  inhomogeneity has the effect of creating a central region of high intensity. In (b), a more homogeneous excitation is achieved. Images courtesy of V.A. Stenger.

- (Transmit-GRAPPA). In: Proceedings of the 13<sup>th</sup> Annual Meeting of ISMRM, 2005; Miami. p 2435.
5. Pruessmann KP, Weiger M, Scheidegger MB, Boesiger P. SENSE: sensitivity encoding for fast MRI. *Magn Reson Med* 1999;42(5):952-962.
  6. Griswold MA, Jakob PM, Heidemann RM, Nittka M, Jellus V, Wang J, Kiefer B, Haase A. Generalized autocalibrating partially parallel acquisitions (GRAPPA). *Magn Reson Med* 2002;47(6):1202-1210.
  7. Pauly J, Nishimura D, Macovski A. A k-space analysis of small-tip-angle excitation. *J Magn Reson* 1989;81:43-56.
  8. Saekho S, Boada FE, Noll DC, Stenger VA. Small tip angle three-dimensional tailored radiofrequency slab-select pulse for reduced B1 inhomogeneity at 3 T. *Magn Reson Med* 2005;53(2):479-484.
  9. Stenger VA, Saekho S, Zhang Z, Yu S, Boada FE. B1 Inhomogeneity Reduction with Transmit SENSE. In: Proceedings of the 2<sup>nd</sup> International Workshop on Parallel MRI, 2004; Zurich. p 94.
  10. Katscher U, Vernickel P, Hanft M. Static and Dynamic RF-shimming in the framework of Transmit SENSE. In: Proceedings of the 13<sup>th</sup> Annual Meeting of ISMRM, 2005; Miami. p 2256.
  11. Stenger VA, Boada FE, Noll DC. Three-dimensional tailored RF pulses for the reduction of susceptibility artifacts in T2\*-weighted functional MRI. *Magn Reson Med* 2000;44(4):525-531.
  12. Zhu Y, Watkins R, Giaquinto R, Hardy C, Kenwood G, Mathias S, Valent T, Denzin M, Hopkins J, Peterson W, Mock B. Parallel Excitation on an Eight Transmit-Channel MRI System. In: Proceedings of the 13<sup>th</sup> Annual Meeting of ISMRM, 2005; Miami. p 14.
  13. Ullmann P, Junge S, Wick M, Seifert F, Ruhm W, Hennig J. Experimental analysis of parallel excitation using dedicated coil setups and simultaneous RF transmission on multiple channels. *Magn Reson Med* 2005;54(4):994-1001.
  14. Yip CY, Fessler JA, Noll DC. Iterative RF pulse design for multidimensional, small-tip-angle selective excitation. *Magn Reson Med* 2005;54(4):908-917.
  15. Sutton BP, Noll DC, Fessler JA. Fast, iterative image reconstruction for MRI in the presence of field inhomogeneities. *IEEE Trans Med Imaging* 2003;22(2):178-188.
  16. Fessler JA. Penalized weighted least-squares image reconstruction for positron emission tomography. *IEEE Trans Med Imaging* 1994;13(4):290-300.
  17. Zhang Z, Stenger VA. Validation of Transmit SENSE with Reciprocity. In: Proceedings of the 13<sup>th</sup> Annual Meeting of ISMRM, 2005; Miami. p 2434.
  18. Noll DC, Meyer CH, Pauly J, Nishimura D, Macovski A. A homogeneity correction method for magnetic resonance imaging with time-varying gradients. *IEEE Trans Med Imaging* 1991;10(4):629-637.
  19. Schneider E, Glover G. Rapid in vivo proton shimming. *Magn Reson Med* 1991;18(2):335-347.
  20. Pauly JM, Nishimura DG, and Macovski A. A linear class of large-tip-angle selective excitation pulses. *J Magnetic Reson*, 82:571-587, 1989.
  21. Chan RH, Ng MK. Conjugate Gradient Methods for Toeplitz Systems. *SIAM Review* 1996;38(3):427-482.
  22. Parker GJ, Barker GJ, Tofts PS. Accurate multislice gradient echo T(1) measurement in the presence of non-ideal RF pulse shape and RF field nonuniformity. *Magn Reson Med* 2001;45:838-845.
  23. Barker GJ, Simmons A, Arridge SR, Tofts PS. A simple method for investigating the effects of non-uniformity of radiofrequency transmission and radiofrequency reception in MRI. *Br J Radiol* 1998;71:59-67.
  24. Wang J, Qiu M, Yang QX, Smith MB, Constable RT. Measurement and Correction of Transmitter and Receiver Induced Nonuniformities In Vivo. *Magn Reson Med* 2005;53:408-417.
  25. Kurpad KN, Boskamp EB, Wright SM. A Parallel Transmit Volume Coil with Independent Control of Currents on the Array Elements. In: Proceedings of the 13<sup>th</sup> Annual Meeting of ISMRM, 2005; Miami. p 16.
  26. Nam H, Wright SM. Transmit Surface Coil Array Using RF Current Sources. In: Proceedings of the 13<sup>th</sup> Annual Meeting of ISMRM, 2005; Miami. p 917.
  27. Yip CY, Fessler JA, Noll DC. A Novel, Fast and Adaptive Trajectory in Three-Dimensional Excitation K-Space. In: Proceedings of the 13<sup>th</sup> Annual Meeting of ISMRM, 2005; Miami. p 2350.